MOLECULAR AND CELLULAR BIOLOGY, Mar. 2008, p. 1503–1514 Vol. 28, No. 5
0270-7306/08/$08.00+0 doi:10.1128/MCB.01565-07

ARS2 Is a Conserved Eukaryotic Gene Essential for Early Mammalian Development▽†

Michael D. Wilson,[1,2]‡ Diana Wang,[1,2,3] Rebecca Wagner,[1] Hilde Breyssens,[4] Marina Gertsenstein,[5] Corrinne Lobe,[6] Xin Lu,[4] Andras Nagy,[5] Robert D. Burke,[1,2,3] Ben F. Koop,[1,2]* and Perry L. Howard[1,2,3]*

Centre for Biomedical Research, University of Victoria, Victoria, British Columbia, Canada[1]; Department of Biology, University of Victoria, Victoria, British Columbia, Canada[2]; Department of Biochemistry and Microbiology, University of Victoria, Victoria, British Columbia Canada[3]; Ludwig Institute for Cancer Research, University of Oxford, Oxford, United Kingdom[4]; Samuel Lunenfeld Research Institute, Mount Sinai Hospital, Toronto, Ontario, Canada[5]; and Sunnybrook Health Sciences Centre, Toronto, Ontario, Canada[6]

Received 26 August 2007/Returned for modification 25 September 2007/Accepted 7 December 2007

Determining the functions of novel genes implicated in cell survival is directly relevant to our understanding of mammalian development and carcinogenesis. *ARS2* is an evolutionarily conserved gene that confers arsenite resistance on arsenite-sensitive Chinese hamster ovary cells. Little is known regarding the function of *ARS2* in mammals. We report that *ARS2* is transcribed throughout embryonic development and is expressed ubiquitously in mouse and human tissues. The mouse ARS2 protein is predominantly localized to the nucleus, and this nuclear localization is ablated in *ARS2*-null embryos, which in turn die around the time of implantation. After 24 h of culture, *ARS2*-null blastocysts contained a significantly greater number of apoptotic cells than wild-type or heterozygous blastocysts. By 48 h of in vitro culture, null blastocysts invariably collapsed and failed to proliferate. These data indicate *ARS2* is essential for early mammalian development and is likely involved in an essential cellular process. The analysis of data from several independent protein-protein interaction studies in mammals, combined with functional studies of its *Arabidopsis* ortholog, *SERRATE*, suggests that this essential process is related to RNA metabolism.

Arsenic contamination, particularly of drinking water, is of worldwide concern, and a variety of diseases and syndromes related to chronic exposure to arsenic are known (reviewed in reference 22). Arsenic is a carcinogen, although its mode of action is still under active investigation (27). Despite its carcinogenicity, arsenic trioxide is used to treat relapsed acute promyelocytic leukemia and can induce complete remission in patients without the myeloid suppression that accompanies other treatments (reviewed in reference 38). The reasons for the increased sensitivity of leukemic cells to arsenic are still being elucidated. *ARS2* (for arsenite resistance gene 2; originally called *ASR2*) confers arsenite resistance on arsenite-sensitive Chinese hamster ovary (CHO) cells (28). *ARS2* resides within a region of human chromosome 7 recurrently deleted in myeloid leukemia (40). However, it is not known whether the loss of *ARS2* contributes to the increased sensitivity of leukemic cells to arsenic.

With the notable exception of *Saccharomyces cerevisiae*, *ARS2* orthologs are found in the genomes of most eukaryotic organisms. The ARS2 protein is highly conserved; within mammals, there is ≥98% amino acid identity. An "ARS2 domain" comprising the last 200 amino acids of the protein (Interpro no. IPR007042; Pfam no. PF04959) has been identified and exclusively assigned to *ARS2* orthologs. A general feature of *ARS2* orthologs is that they encode a single C_2H_2-like zinc finger domain in which one of the cysteines has been lost in metazoans. There are also multiple bipartite nuclear localization motifs (25), which suggests that the protein may function in the nucleus. Despite its potential involvement in arsenite resistance, its location in a genomic region commonly deleted in acute myeloid leukemia, and its conservation in eukaryotic organisms, little is known about the function of mammalian *ARS2*.

In plants, *ARS2* is a developmental regulator. The *Arabidopsis ARS2* ortholog is known as *SERRATE* (*SE*), and *se* mutants develop pleiotropic abnormalities during shoot development, indicating that it is involved in plant organogenesis (5, 13, 24, 25, 32). Overexpression of *SERRATE* causes accelerated plant growth (increased leaf production and shorter time to flowering) (25). *ARS2* is also essential in zebrafish. In a large-scale zebrafish insertional-mutagenesis project, three independent retroviral insertions occurred in *ARS2*. One of these mutations was bred to homozygosity and resulted in an embryonic-lethal phenotype with multiple abnormalities, including central nervous system and body necrosis, small head and eyes, and pericardial edema (1, 11).

Uncovering the functions of genes implicated in the cellular response to arsenic is of interest, as arsenic is used to treat promyelocytic leukemia and is being considered asa treatment for other cancers (37). Developmental phenotypes caused by

* Corresponding author. Mailing address: Centre for Biomedical Research, University of Victoria, P.O. Box 3020 Station CSC, Victoria, BC, Canada V8W 3N5. Phone for P. Howard: (250) 472-4074. Fax: (250) 472-4075. E-mail: phoward@uvic.ca. Phone for B. F. Koop: (250) 472-4067. Fax: (250) 472-4075. E-mail: bkoop@uvic.ca.

‡ Present address: Cancer Research UK, Cambridge Research Institute, Cambridge, United Kingdom.

† Supplemental material for this article may be found at http://mcb.asm.org/.

▽ Published ahead of print on 17 December 2007.

mutations of *ARS2* orthologs in zebrafish and *Arabidopsis*, its presence in diverse eukaryotic genomes, and its high sequence identity between species suggest that *ARS2* has essential functions. For these reasons, we investigated the role of *ARS2* in mammals by characterizing its expression in mouse and human tissues and ablating its expression through targeted disruption in the mouse genome.

MATERIALS AND METHODS

Northern blot analysis. A 314-bp mouse *ARS2* probe was amplified by PCR from a full-length *ARS2* clone (BC066831), using the primers Ars2_1180F and Ars2_pet30_XhoR (see Table SA1 in the supplemental material). An 880-bp human *ARS2* probe was amplified from human liver first-strand cDNA using the primers hARS2_3F and hARS2_exon9R (BD Biosciences). Both probes were gel purified prior to random primer labeling with [α^{32}P]dCTP, using the RediPrime kit (Amersham). The mouse and human probes were hybridized overnight at 65°C to commercially prepared Northern blots of mouse and human poly(A)$^+$ RNA, respectively, using the manufacturer-supplied ExpressHyb hybridization solution (mouse MTN blot no. 7762-1 and human 12-lane MTN blot no. 7780-1; BD Biosciences). After hybridization, the blots were washed twice in 2× SSC (1× SSC is 0.15 M NaCl plus 0.015 M sodium citrate)-0.1% sodium dodecyl sulfate (SDS) at room temperature for 15 min each, followed by two 15-min washes in 0.1× SSC-0.1% SDS performed at 65°C. The blots were visualized using a Storm phosphorimager (Molecular Dynamics).

cDNA expression studies. Mouse and human expression studies of *ARS2* were carried out on Clontech multiple tissue panels (BD Biosciences) using HotStarTaq DNA polymerase (Qiagen). A 50-μl volume was used for all expression studies, and the cycling parameters were as follows: 95°C for 15 min for *Taq* activation and eight cycles of 94°C for 30 s, 65°C for 1 min, and 72°C for 1 min, followed by 30 to 33 cycles of 94°C for 30 s, 58°C for 1 min, and 72°C for 1 min and a final extension of 5 min at 72°C. The mouse *ARS2* PCR was performed using the primers ARSupstrF and Ars_mus1R, which amplified the expected 1,890-bp product. The human *ARS2* PCR was performed with ARSupstrF and hARS-9R1, which amplified an expected 1,925-bp product. The PCR products from the cDNA were verified by DNA sequencing.

RNA blotting. Human RNA master blots from Clontech contain 50 human poly(A)$^+$ RNA samples that have been normalized to the mRNA expression levels of eight different genes. RNA blots were hybridized with the same probe used for Northern blotting. Both probes were randomly labeled with [α-^{32}P]dCTP using the RediPrime random primer labeling kit (Amersham). The *ARS2 5′* probe was hybridized overnight using ExpressHyb hybridization solution at 65°C. The blot was washed according to the manufacturer's protocol.

Production and characterization of anti-ARS2 antibodies. Antibodies were generated using the longest human ARS2 clone, BC069249. This clone is missing the first 64 amino acids of the predicted full-length ARS2 protein (40). Monoclonal and polyclonal antibodies were raised to the region corresponding to the N terminus of BC069249 (amino acids 65 to 370) and were designated LX186.3 and XL12.2, respectively.

ARS2 protein expression. The complete coding region of *ARS2* (2,628 bp) was PCR amplified from the full-length mouse *ARS2* clone (BC066831) using Platinum *Pfx* DNA polymerase (Invitrogen). All vector inserts were confirmed to be mutation free by DNA sequencing. The full-length *ARS2* gene was cloned in frame into a retroviral vector derived from the pMSCVpuro vector (BD Biosciences) but modified to contain an N-terminal three-FLAG sequence (derived from the p3XFLAG-CMV vector [Sigma]). The full-length *ARS2* coding sequence was amplified using the restriction enzyme-modified PCR primers Ars2_MSCVpacF and Ars2_MSCVpacR. A C-terminal Myc-His fusion protein was created by cloning the full-length *ARS2* product into the mammalian expression vector pcDNA3.1/Myc-His(−) A vector (Invitrogen) using the restriction site-modified primers Ars2_mycF and Ars2_mycR.

Stable cell lines expressing ARS2 were generated using the human kidney-derived cell line BOSC-23 (ATCC CRL 11270) transfected with the 3XFLAG-ARS2 or ARS2-Myc-His vector. The vector (10 μg) was added to 1.5 ml of serum-free Dulbecco's modified Eagle's medium (DMEM) and mixed with an additional 1.5 ml serum-free DMEM containing 40 μl of transfectin (Bio-Rad). This transfection mixture was then added to BOSC-23 cells. Selection for successful transfection events was performed with puromycin (25 μg/ml). The cells were maintained until they reached near confluence and individual colonies were visible. Colonies were pooled and lysed in PLC lysis buffer (50 mM HEPES, pH 7.5, 150 mM NaCl, 10% glycerol, 1% Triton, 1 mM EGTA, 1.5 mM $MgCl_2$). After cell lysis, the debris was pelleted (14,000 × g; 10 min) and the supernatant was retained for Western blotting.

Western blotting. Cell lysates were separated by SDS-polyacrylamide gel electrophoresis (10%), followed by transfer to a polyvinylidene difluoride membrane. The membrane was blocked with 5% nonfat milk (NFM) in Tris-buffered saline–Tween 20 (0.5%) (TBST) for 2 h. The 3XFLAG-ARS2 was detected with the primary anti-FLAG M2 antibody (Stratagene) used at 0.5 μg/ml in 3% NFM overnight at 4°C. The ARS2-Myc-His tag protein was detected with an anti-Myc antibody (Santa Cruz Biotechnology) used at 1:400 dilution. After being washed with TBST, the blots were incubated with the secondary anti-mouse horseradish peroxidase-conjugated antibody diluted 1:10,000 in TBST containing 3% NFM. After being washed in TBST, the blots were developed using the ECL-plus kit (Amersham) according to the manufacturer's protocol.

Targeted disruption of *ARS2* in R1 ES cells and mouse production. The *ARS2* containing mouse chromosome 5 BAC 423o3 (AF312033 [40]; CITB-CJ7-B mouse library derived from the 129Sv/J mouse strain; Research Genetics, Huntsville, AL) was digested with SpeI, and the 8,418-bp fragment was subcloned into the XbaI site of the osdupde1 vector (kindly provided by Oliver Smithies). The 1,702-bp short arm was amplified by PCR using Asr_20580_NheI and Asr_22282_XhoI primers and Vent polymerase (New England Biolabs). The fragment was digested and cloned into the NheI and XhoI sites of osdupdeI and verified by PCR and DNA sequencing of vector/insert junctions. The targeting vector was linearized using NotI and electroporated into 129S1/Sv-derived R1 embryonic stem (ES) cells (21) at a concentration of ~2 μg per million cells. Electroporation was done in electroporation buffer (Specialty Media) using a Bio-Rad GenePulsar set at 250 V and 500 μF. The electroporated cells were plated on gelatinized plates as previously described (20). G418 (150 μg/ml) was added 24 h after the electroporation; 48 h after the electroporation, FIAU (5-iodo-2′-fluoro-2′deoxy-1-β-D-arabino-furanosyl-uracil) was added to the ES-DMEM at a concentration of 0.2 μM. After 7 days of selection, 192 isolated colonies were picked and grown up individually on two 96-well plates. DNA preparations were performed in the 96-well plates as previously described (26).

Electroporation of the vector construct into R1 ES cells yielded 11 positive ES cell clones that showed the predicted band size shifts when analyzed by Southern blotting. These 11 clones were expanded, and the Southern blot analysis was repeated using BamHI and the short-arm probe. The BamHI-digested wild-type band detected by this probe was 9,579 bp in length, and the mutant band was 5,658 bp. Further analysis was performed by EcoRI digestion in combination with the long-arm probe to ensure a correct long arm. EcoRI-digested genomic DNA produced a 14,786-bp band (wild type) or a mutant 11,997-bp band. The BamHI Southern blots were also probed with the neomycin cassette to confirm that a single integrant was obtained. From this analysis, two clones were chosen to make aggregation chimeras (A4-E1 and A4-G6).

Aggregation chimeras. Cleavage stage Crl:CD1(ICR) and129S2/SvPasCrl embryos (Charles River, Canada) were aggregated with correctly targeted ES clones using the established procedure (16). Germ line transmission was obtained for ES cell clones A4-E1 and A4-G6. Chimera mice were bred to both 129S2/SvPasCrl and Crl:CD1(ICR) backgrounds (Charles River, Canada). Initial characterization of the knockout mice was carried out on both strains using both cell lines. Cre-mediated excision of the *neo* cassette from the Ars-E1 line (ARS2$^{\Delta neo}$) was achieved by crossing the Ars-E1 line with the *pCX-NLS-Cre* line (19). Southern blot analysis of ARS2$^{\Delta neo/+}$ mice was performed as described above with BamHI digestion that produced a 4.4-kb mutant band. We cryopreserved two ARS2$^{+/\Delta neo}$ lines designated 129S2/SvPasCrl-*Ars2*^{tm1BFK} and 129S2/SvPas/CD1Crl-*Ars2*^{tm1BFK}.

PCR genotyping. PCR genotyping was performed on embryos and ear punches that had been digested at 55°C (4 h to overnight) in 10 to 100 μl ear punch buffer (50 mM KCl, 10 mM Tris HCl, pH 8.3, 2.0 mM $MgCl_2$ 0.1 mg/ml gelatin, 0.45% Nonidet P-40, 0.45% Tween 20) containing 0.5 mg/ml proteinase K. The genotyping PCR was performed in 25-μl reaction mixtures using the manufacturer-supplied 10× reaction buffer containing 10 mM $MgCl_2$. Each reaction mixture contained 0.48 μM (final concentration) of each primer, 10× deoxynucleoside triphosphate stock consisting of 2 mM of each deoxynucleoside triphosphate and 0.625 unit of HotStarTaq (Qiagen). Primers Ars2_27244F and Ars2_27576R amplify a wild-type 333-bp band. Ars2_21942F and the vector-derived primer 5066R amplify a 563-bp band that detects the *ARS2* locus mutated with the *neo* cassette. Both primer sets were used simultaneously in the same reaction. The cycling parameters for all PCR genotyping assays were as follows: 95°C for 15 min for *Taq* activation and 40 cycles of 94°C for 20 s, 58°C for 1 min, 72°C for 1 min, and a final extension of 5 min at 72°C.

Isolation and culture of mouse embryos. Timed natural matings between ARS2$^{+/-}$ mice were used to obtain embryos. The time of detection of the vaginal plug was designated embryonic day 0.5 (E0.5). Blastocysts were collected at E3.5

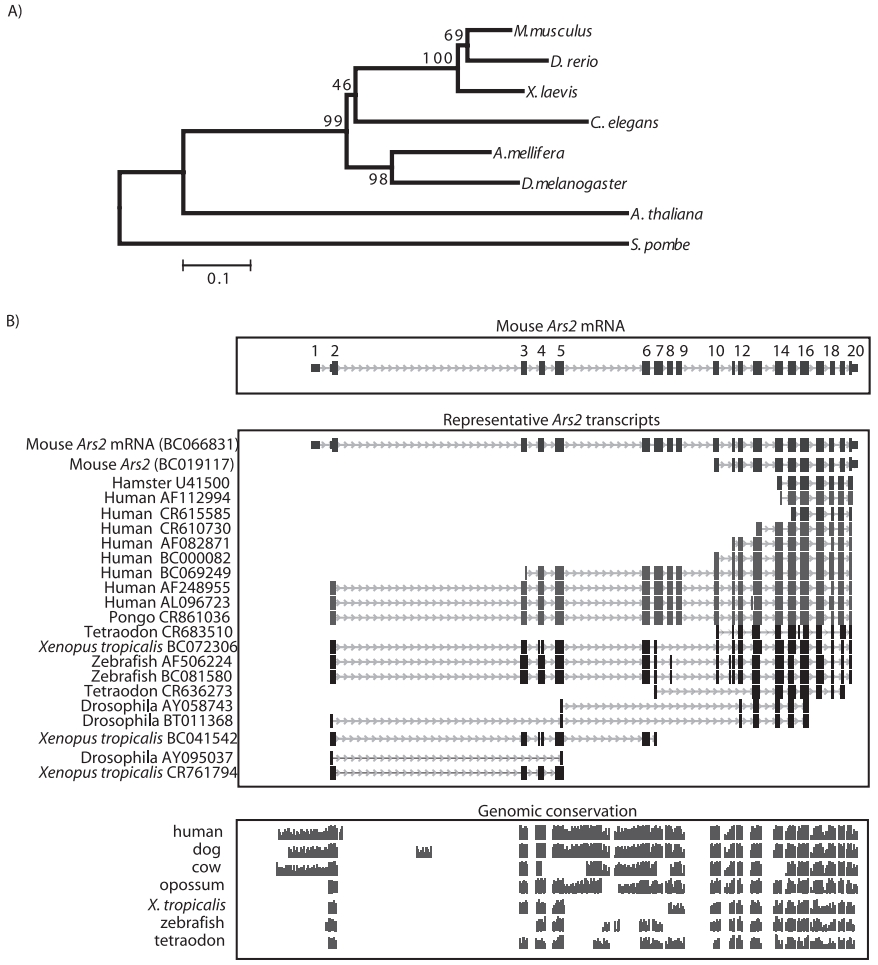

FIG. 1. Overview and evolution of ARS2. (A) Phylogenetic analysis of the *ARS2* genes from representative eukaryotic species. Amino acid alignments were made using CLUSTALW and manually edited. Columns containing gaps were deleted, and 224 informative sites were used to construct the phylogeny. A neighbor-joining tree using a Poisson distance matrix was made. (B) Alignment of the mouse *ARS2* locus with representative mRNAs and genomic DNAs. Representative mRNAs and ESTs were prealigned by the University of California Santa Cruz using the BLAT algorithm. Genomic conservation of the *ARS2* gene between mouse and seven additional species is shown as vertical black lines. The alignments were precomputed using the Multiz align algorithm (3) and can be found at positions chr5:136,243,845 to 136,260,875 of the mouse March 2005 assembly on the UCSC genome browser website.

by flushing the uteri with M2 medium (Sigma) supplemented with antibiotics. The blastocysts were transferred to gelatin-coated 96-well, 4-well, or chambered glass coverslips containing ES-DMEM with or without leukemia inhibitory factor (LIF). Treatment with acid Tyrode's solution was used to remove the zona pellucida in some experiments. The embryos were photographed every 24 h using a Nikon Diaphot microscope and ImageJ software. Embryos between E6.5 and E7.5 were carefully dissected in M2 medium or cold phosphate-buffered saline (PBS), rinsed several times, and then genotyped by PCR. Photographs were taken using an Olympus SZX9 microscope. Most intercrosses used to obtain E6.5 to E7.5 embryos were performed between ARS2$^{+/neo}$ and ARS2$^{+/\Delta neo}$ mutants, since the detection of embryos with three alleles (*ARS2*^{neo}, *ARS2*$^{\Delta neo}$, and *ARS2* wild type) would serve as an indicator of maternal contamination in the genotyping assay. Individual implantations of E5.5 and E7.5 litters were fixed at 4°C overnight in 4% paraformaldehyde (PFA), embedded in Epon, serially sectioned, and stained with Richardson's blue stain.

Immunofluorescence. Blastocysts were fixed in ice-cold 4% PFA for 2 minutes at room temperature. Permeabilization was performed with PBS–0.5% Triton X-100 for 30 min at room temperature. The blastocysts were rinsed extensively with PBS–0.1% Triton X-100 containing 6 mg/ml bovine serum albumin. Blocking was done for 1 h at room temperature in 10% lamb serum in PBS–0.1% Triton X-100. The following primary commercial antibodies were used: anti-OCT4 (polyclonal; Santa Cruz Biotechnology; sc-9081), anti-CDX2 (monoclonal; BioGenex; CDX2-88), anti-histone H3 (phospho-S10) (monoclonal; Abcam; ab5176), anti-FLAG, and anti-Myc. Alexa Fluor 488 goat anti-mouse immunoglobulin G (IgG) (1/400) and Alexa Fluor 568 goat anti-rabbit IgG (1/1,200) were used as secondary antibodies in PBS–0.1% Triton X-100. The nuclear morphology was visualized using the far-red dye DRAQ5 (1:500 in PBS plus 0.1% Triton X-100; BioStatus Ltd.). Embryos were imaged using the Eclipse T-E2000-U Nikon confocal laser scanning microscope. Cell counting was performed using Imaris software (Bitplane AG) in combination with manual verification of the automated results.

TUNEL assay. Terminal deoxynucleotidyltransferase-mediated dUTP fluorescein nick end labeling (TUNEL) assays were performed on E3.5 blastocysts using the In Situ Cell Death Detection kit (Roche). Blastocysts were cultured for 24 h in ES-DMEM without LIF and fixed in ice-cold 4% PFA for 10 min at room temperature. The blastocysts were rinsed with PBS-0.1% Tween 20 containing 6 mg/ml bovine serum albumin. Permeabilization was done for 10 min at room temperature in PBS, 0.5% Triton X-100, 0.1% sodium citrate. The embryos were rinsed again several times and then incubated with the fluorescein-dUTP and terminal deoxynucleotidyltransferase enzyme for 1 h at 37°C. Positive controls consisting of blastocysts treated with DNase and negative controls, in which the terminal deoxynucleotidyltransferase enzyme was omitted, were included for every experiment. Nuclei were labeled with DRAQ5 for 30 min (1:500 in PBS–0.1% Tween 20) and transferred to slides. The embryos were imaged using confocal laser microscopy and then genotyped by PCR.

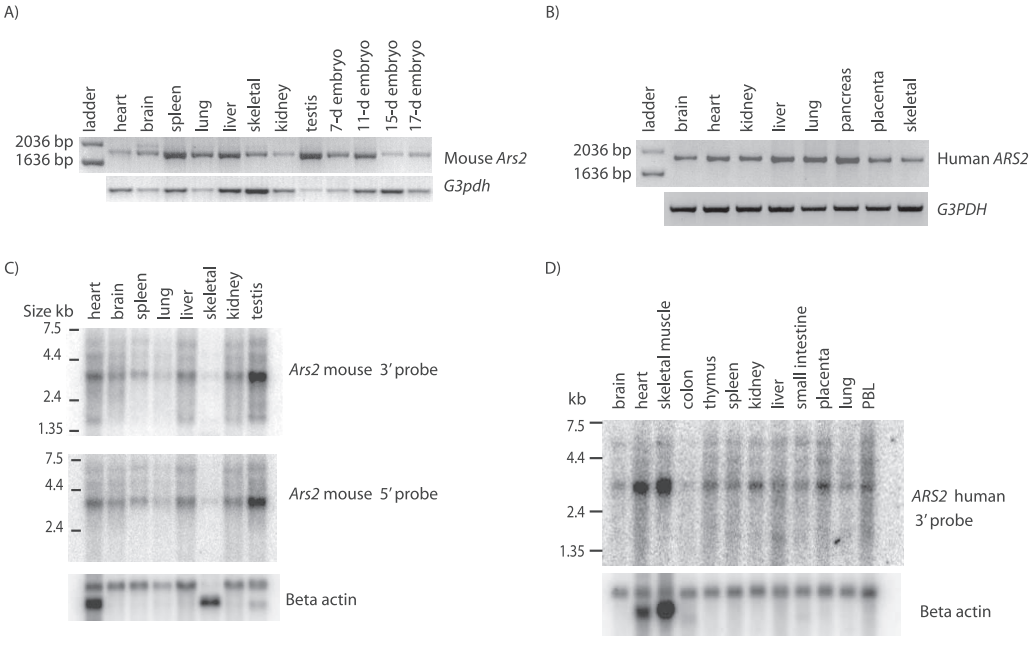

	1	2	3	4	5	6	7	8
A	whole brain	amygdala	caudate nucleus	cerebellum	cerebral cortex	frontal lobe	hippocampus	medulla oblongata
B	occipital pole	putamen	substantia nigra	temporal lobe	thalamus	subthalamic nucleus	spinal cord	
C	heart	aorta	skeletal muscle	colon	bladder	uterus	prostate	stomach
D	testis	ovary	pancreas	pituitary gland	adrenal gland	thyroid gland	salivary gland	mammary gland
E	kidney	liver	small intestine	spleen	thymus	peripheral leukocyte	lymph node	bone marrow
F	appendix	lung	trachea	placenta				
G	fetal brain	fetal heart	fetal kidney	fetal liver	fetal spleen	fetal thymus	fetal lung	
H	yeast total RNA	yeast tRNA	E. coli rRNA	E. coli DNA	Poly r(A)	human C0t DNA	human DNA	human DNA

FIG. 2. Expression analysis of mouse and human *ARS2* mRNAs. (A and B) Semiquantitative PCR analysis of normalized first-strand cDNAs in mouse and human tissues. The mouse 1,890-bp ARS2 product was observed in all tissues, and a mouse *G3pdh* primer set was used as a positive control. (C) Mouse *ARS2* Northern blot. (Top) Normalized mouse Northern blot tissues probed with the ARS2 3′ probe. (Middle) Northern blot probed with the ARS2 5′ probe. (Bottom) Beta actin control probe. (D) (Top) Human *ARS2* Northern blot probed with the *ARS2* human 3′ probe. (Bottom) Northern blot probed with beta actin. (E) Normalized RNA blot of multiple human tissues using the ARS2 5′ cDNA as a probe.

RESULTS

Conservation and mRNA expression of *ARS2*. We and others have previously shown that *ARS2* is conserved in mammals and plants (25, 40). Further analysis of eukaryotic genome assemblies and expressed sequence tags (ESTs) suggests that there is a single *ARS2* homolog in most eukaryotic genomes (Fig. 1). This suggests that *ARS2* arose early in eukaryotic evolution and that it may serve a basic cellular function.

Conservation between mouse *ARS2* and its orthologs can be observed at both the mRNA and genomic-sequence levels (Fig. 1B) (25, 40). We examined the expression of *ARS2* in mouse and human tissues by PCR and Northern blotting analysis. By PCR, *ARS2* was expressed in all mouse and human tissues tested (Fig. 2). Evidence of a slightly larger mouse transcript variant (~150 bp) can be seen in most tissues (Fig. 2A) and may represent previously described alternative splice variants of *ARS2* (40). To determine *ARS2* transcript size, relative abundance, and distribution in both mouse and human tissues, Northern blot analysis was performed. *ARS2* showed ubiquitous expression, with the highest levels in mouse testes, heart, and liver and human heart and skeletal muscle (Fig. 2C and D). The predominant transcript size of ~3.0 kb corresponds to the full-length mouse cDNA sequence (BC066831) that is predicted to encode a 100-kDa protein product. With the 3′ probe, smaller weak bands could be seen at ~2 kb and 1 kb. These products likely represent *ARS2* isoforms generated from internal promoters, as smaller C-terminal transcripts have been identified in human, mouse, *Drosophila*, and Chinese hamster (Fig. 1B). Interestingly, the original arsenite resistance *ARS2* cDNA from CHO cells was a C-terminal isoform containing the ARS2 domain. This suggests that C-terminal messages may be functionally relevant. An expanded screen of a normalized RNA dot blot of 50 human tissues confirmed that ARS2 is ubiquitously expressed, with the highest levels of expression in the testes, fetal lung, placenta, pituitary gland, bone marrow, thymus, and prostate (Fig. 2E).

We also examined *ARS2* expression during mouse development. *ARS2* is expressed at E7, E11, E15, and E17 (Fig. 2A).

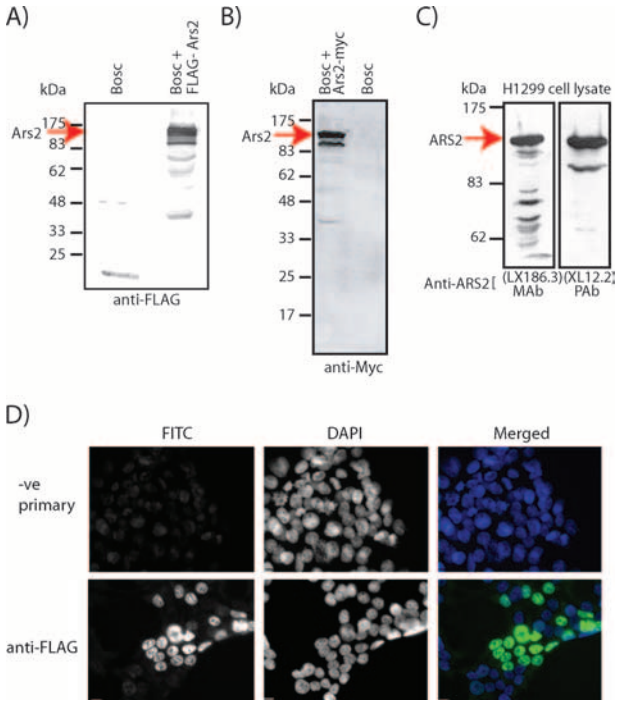

FIG. 3. ARS2 is expressed predominantly as a 100-kDa protein. (A to C) Western blot analysis of N terminus FLAG tag full-length mouse ARS2 protein stably transfected into the BOSC kidney cell line (A), C terminus MYC full-length mouse ARS2 fusion protein (transient transfection of BOSC cells) (B), and H1299 cell lysate using polyclonal and monoclonal anti-ARS2 antibodies raised against human ARS2 (C). (D) Anti-FLAG antibody staining of three-FLAG N-terminally labeled mouse ARS2 in a stably transfected BOSC cell line and a negative control in which the primary FLAG antibody was omitted (−ve primary). FITC, fluorescein isothiocyanate; DAPI, 4′,6′-diamidino-2-phenylindole.

In addition, the distribution of *ARS2* transcripts observed in the mouse EST database is biased toward prenatal stages. For example, 165 *ARS2* transcripts that were derived directly from mouse tissues (not including cancer cell lines) are found in the EST database. Ninety of the 165 ESTs can be assigned to a prenatal developmental stage (preimplantation through late gestation). When these EST counts were normalized to reflect the total number of transcripts derived from each tissue-specific library, 480 *ARS2* transcripts per million were found to be derived from prenatal tissue compared to 275 transcripts per million derived from postnatal tissue (39). Within the prenatal tissues, preimplantation expression is most dominant and includes ES cells and trophoblast cells.

Protein expression of mouse and human ARS2. The full-length mouse *ARS2* cDNA produced the predicted 100-kDa full-length protein when expressed as an N terminus three-FLAG fusion protein (Fig. 3A) and as a C terminus Myc-His fusion protein (Fig. 3B). Polyclonal and monoclonal antibodies raised against ARS2 gave a predominant 100-kDa band and a less intense 90-kDa band in human H1299 cell line lysates (Fig. 3C). Both the N- and C-terminal full-length ARS2 fusion proteins showed similarly sized smaller bands when expressed in BOSC cells, suggesting this band may be a product of proteolytic degradation. ARS2 contains multiple nuclear localization signals and a zinc finger-like domain, which suggests ARS2 may function in the nucleus. Strong nuclear localization, with weak cytoplasmic staining, was detected using anti-FLAG antibodies in FLAG-ARS2-expressing cell lines (Fig. 3D).

***ARS2* is essential for early development.** To elucidate the role of *ARS2* in mammals, a gene-targeting vector was designed to remove the mouse *ARS2* putative promoter to, and including part of, the third exon (Fig. 4A and B). In addition to the conserved proximal promoter region, this deletion removed the first 49 amino acids of ARS2, which are conserved throughout the *Eukaryota*. Germ line transmission was obtained for the independent ES cell clones A4-E1 and A4-G6 (Fig. 4C). Initial characterization of the knockout mice was carried out on both 129S2/SvPasCrl and Crl:CD1(ICR) background strains using mice derived from both cell lines. Cre-mediated excision of the *neo* cassette from the Ars-E1 line was achieved by crossing the Ars-E1 line with the *pCX-NLS-Cre* line (19). Southern blot analysis of $ARS2^{+/\Delta neo}$ mice produced the expected 4.4-kb mutant band (Fig. 4D). Analysis was carried out on the $ARS2^{+/neo}$ and $ARS2^{+/\Delta neo}$ lines. As there were no phenotypic differences between the $ARS2^{+/neo}$ and $ARS2^{+/\Delta neo}$ lines, the heterozygous *ARS2* mutant allele is referred to as $ARS2^{+/-}$ hereafter.

Breeding of $ARS2^{+/-}$ mice produced no homozygous $ARS2^{-/-}$ offspring for either of the stem cell-derived lines (Ars-E1 or Ars-G6) after 28 and 16 intercrosses, respectively (Table 1). No significant ($P \leq 0.05$) deviation from the expected 1:2 Mendelian wild-type-to-heterozygous ratio was detected (χ^2 [1, $n = 129$] = 1.71; $P = 0.25$). $ARS2^{+/-}$ mice were healthy and showed no obvious differences from their wild-type littermates (data not shown).

Yolk sacs from E10.5 and E12.5 embryos obtained from $ARS2^{+/-}$ intercrosses were genotyped by Southern blotting, and no $ARS2^{-/-}$ embryos were detected (Fig. 4E). PCR genotyping of E6.5 and E7.5 embryos failed to identify any $ARS2^{-/-}$ embryos (Table 1). However, approximately 18% of deciduas from embryos dissected at E6.5 and E7.5 were small and devoid of embryos (Fig. 5A). Serial sectioning of E7.5 deciduas revealed no evidence of the embryo proper in these smaller deciduas (Fig. 5B). Serial sectioning of litters from E5.5 identified small botryoid (grape-like) clusters of abnormal cells with pycnotic nuclei (Fig. 5C). This suggests that a majority of $ARS2^{-/-}$ embryos implant but die around E5.5 (Table 1).

***ARS2*-null embryos are unable to expand in vitro.** $ARS2^{-/-}$ blastocysts were detected at day E3.5 by PCR analysis in Mendelian ratios (χ^2 [2, $n = 85$] = 2.86; $P = 0.24$) (Fig. 4F). To further investigate this early embryonic lethality, we cultured E3.5 blastocysts under conditions used to derive ES cells. To determine the expression of ARS2 in blastocysts, we performed immunofluorescence analysis on wild-type, heterozygous, and homozygous cultured embryos. Both monoclonal (LX186.3) and polyclonal (XL12.2) anti-ARS2 antibodies showed strong nuclear localization and diffuse cytoplasmic staining in all cells of cultured $ARS2^{+/-}$ and $ARS2^{+/+}$ E3.5 embryos and a lack of nuclear localization in $ARS2^{-/-}$ E3.5 embryos (Fig. 6; data not shown for XL12.2). The localization of ARS2 in embryos was consistent with FLAG-ARS2 localization in BOSC cells and confirms that ARS2 is enriched within the nucleus. ARS2-null blastocysts did not adhere well

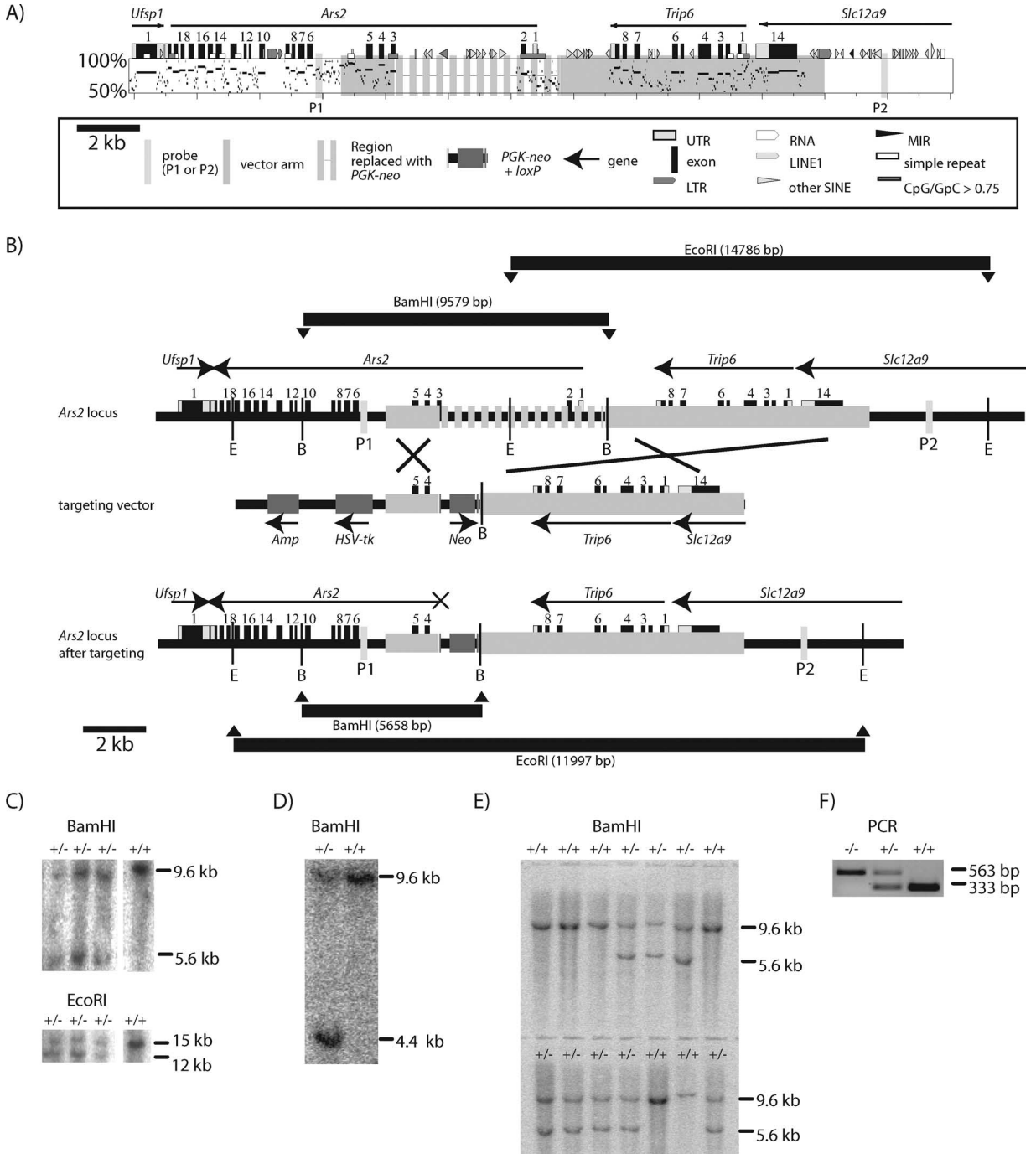

FIG. 4. Gene targeting of mouse *ARS2*. (A) Mouse *ARS2* genomic locus and surrounding genes. Mouse exon positions, repetitive elements, neighboring genes, and thelocations of the arms of homology for gene targeting are shown to scale on the *x* axis. Percent identity shared with the orthologous human locus is shown on the *y* axis. The coordinates are based on the sequence AF312033. (B) Removal of the proximal promoter and exons 1 to 3 of mouse *ARS2* using homologous recombination. Southern blot probes for BamHI and EcoRI digests are labeled P1 and P2, respectively. The targeting vector with a neomycin cassette (*neo*) and herpes simplex virus thymidine kinase (*HSV-tk*) are indicated, along with the arms of homology. (C) Southern blot screening of R1 ES cells: BamHI digestion and P1 produced a wild-type band of 9.6 kb and a mutant band of 5.6 kb, and EcoRI digestion and P2 produced a wild-type band of 14.7 kb and a mutant band of 12.0 kb. (D) Southern blot analysis of the ARS2 locus using BamHI and P1 after Cre-mediated removal of the *neo* cassette. (E) Southern blot analysis of E12.5 yolk sacs from two intercrosses of $ARS2^{+/-}$ mice using BamHI and P1. (F) PCR genotyping of blastocysts (E3.5) from $ARS2^{+/-}$ intercrosses. The wild-type band is 333 bp, and the mutant band is 563 bp.

to the gelatinized-medium dish and did not normally hatch from their zona pellucida. *ARS2*-null blastocysts were noticeably smaller after 24 h in culture and invariably collapsed by 48 h of culture (Fig. 7). Even with the zona pellucida removed, *ARS2*-null embryos did not expand. After 120 h, a small mass of cells remained that showed severe membrane blebbing and abnormal morphology (Fig. 7). The mutant phenotype was the same regardless of the addition of LIF to the media. ARS2

TABLE 1. Breeding analysis of $ARS2^{+/-}$ intercrosses

Age	No. of *ARS2* genotype:		
	+/+	+/−	−/−
28 days	75	111	0
E13.5	3	9	0
E12.5	6	8	0
E10.5	1	9	0
E8.5	1	5	0
E7.5	16	45	0
E7.0	0	6	0
E6.5	3	5	0
E3.5	27	42	16

showed nuclear localization in $ARS2^{+/+}$ and $ARS2^{+/-}$ E3.5 embryos before and after 24 and 48 h of in vitro culture (Fig. 6). A lesser amount of nuclear-localized ARS2 was observed in $ARS2^{-/-}$ embryos at E3.5. This nuclear localization was lost after 24 h of culture and coincided with the onset of the mutant phenotype (Fig. 6). Both serial sectioning of E5.5 embryos and culturing of E3.5 embryos suggested that the embryonic-lethal phenotype begins as early as E4.5 and is fully penetrant by E5.5.

ARS2-null embryos are able to initiate the decidual reaction even though they generally do not hatch from their zona pellucida in vitro. To further investigate the ability of *ARS2* mutants to undergo trophectoderm differentiation, we looked at the trophectoderm-specific expression marker Cdx2 and the inner cell mass (ICM)-restricted marker Oct4. Embryos from $ARS2^{+/-}$ intercrosses were cultured for 48 h and analyzed using immunofluorescence and confocal microscopy. $ARS2^{-/-}$ embryos maintain an outer layer of Cdx2-positive cells and an ICM that is Oct4 positive ($n = 2$). Some polar and mural trophectoderm cells did show either Oct4 or Cdx2 expression, and in those cases, condensed nuclei indicative of apoptosis were observed (Fig. 8). Overall, this suggests that the embryonic-lethal phenotype is not due to a lack of differentiation in early embryonic lineages.

To investigate the possibility of apoptosis in $ARS2^{-/-}$ embryos, we cultured E3.5 embryos for 24 h and identified cell death using the fluorescent TUNEL assay. Excessive apoptosis was observed in $ARS2^{-/-}$ embryos ($n = 7$; mean [M] = 6.7; standard deviation [SD] = 2.5) compared to $ARS2^{+/+}$ and $ARS2^{+/-}$ embryos ($n = 12$; $M = 1.5$; SD = 1.4) (Fig. 9A and B). This difference was statistically significant by the Student t test ($t[28] = 7.4$; $P < 0.0001$). Cell numbers were significantly decreased ($t[38] = 2.3$; $P = 0.0283$) in $ARS2^{-/-}$ embryos ($n = 17$; $M = 79.6$; SD = 15) compared to $ARS2^{+/+}$ and $ARS2^{+/-}$ embryos ($n = 23$; $M = 91.9$; SD = 18) (Fig. 9). The mitotic indices between $ARS2^{+/+}$, $ARS2^{+/-}$, and $ARS2^{-/-}$ embryos were not significantly different ($t[10] = 1.45$; $P = 0.177$) in $ARS2^{-/-}$ embryos ($n = 6$; $M = 3.7$; SD = 1.7) and $ARS2^{+/+}$ and $ARS2^{+/-}$ embryos ($n = 6$; $M = 2.6$; SD = 1.0) (Fig. 9D).

DISCUSSION

Understanding the functions of genes involved in arsenic-related toxicity and chemotherapy is an ongoing challenge. To elucidate the effect of arsenic on cells, Rossman and Wang (28) looked for genes that conferred arsenite resistance on arsenite-sensitive CHO cells by screening a cDNA library made from arsenite-resistant cells (28). From this screen, *Asr2* (*ARS2*), a gene of unknown function, was identified. Here, we show that *ARS2* orthologs are found in almost all eukaryotes; that in mammals, *ARS2* is a ubiquitously expressed gene that encodes a nuclear-localized protein; that *ARS2* is essential for early embryonic development; and that the ablation of the ARS2 protein leads to excessive apoptosis in the early embryo.

While we obtained Mendelian ratios of $ARS2^{-/-}$ blastocysts at E3.5, the lack of expansion of presumptive $ARS2^{-/-}$ embryos in vitro, the presence of empty deciduas at E7.5, and the small degenerate embryos detected at E5.5 indicate that $ARS2^{-/-}$ embryos die around the time of implantation. We conclude that the removal of the conserved upstream region and the first three exons was sufficient to cause the early embryonic lethality. A relatively small amount of nuclear-localized ARS2 could be observed in uncultured $ARS2^{-/-}$ E3.5 embryos compared to heterozygous or wild-type embryos. This nuclear localization was reduced to background levels after 24 h of culture, which corresponds to the onset of the mutant phenotype. As observed after the disruption of many other

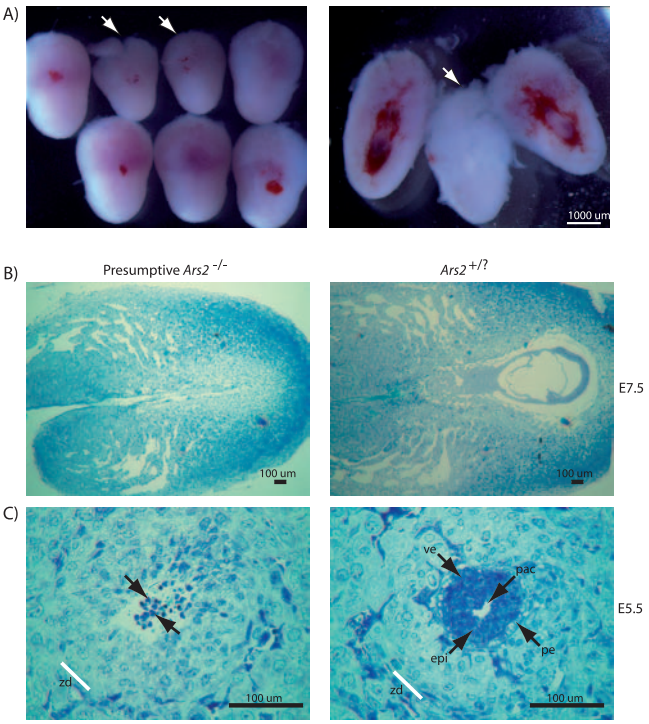

FIG. 5. Dissections and histological analysis of wild-type and presumptive $ARS2^{-/-}$ embryos at E7.5 and E5.5. (A) Representative example of relatively small deciduas routinely obtained from $ARS2^{+/-}$ intercrosses at E7.5 (arrows). Embryos were never recovered from within these deciduas or small deciduas from E6.5. (B) Serial sectioning of random large and small deciduas at E7.5 revealed no discernible embryonic structure in presumptive mutants ($n = 2$). (C) Transverse, serial sectioning of E5.5 implantations from $ARS2^{+/-}$ intercrosses revealed a clear outer boundary of the outer zone of the decidual reaction (zd) in both presumptive $ARS2^{-/-}$ and $ARS2^{+/?}$ embryos. A small mass of abnormal cells with pycnotic nuclei was characteristic of presumptive $ARS2^{-/-}$ embryos ($n = 3$). Wild-type morphology containing a visceral endoderm (ve), parietal endoderm (pe), epiblast (epi), and proamniotic cavity was observed for all $ARS2^{+/?}$ embryos.

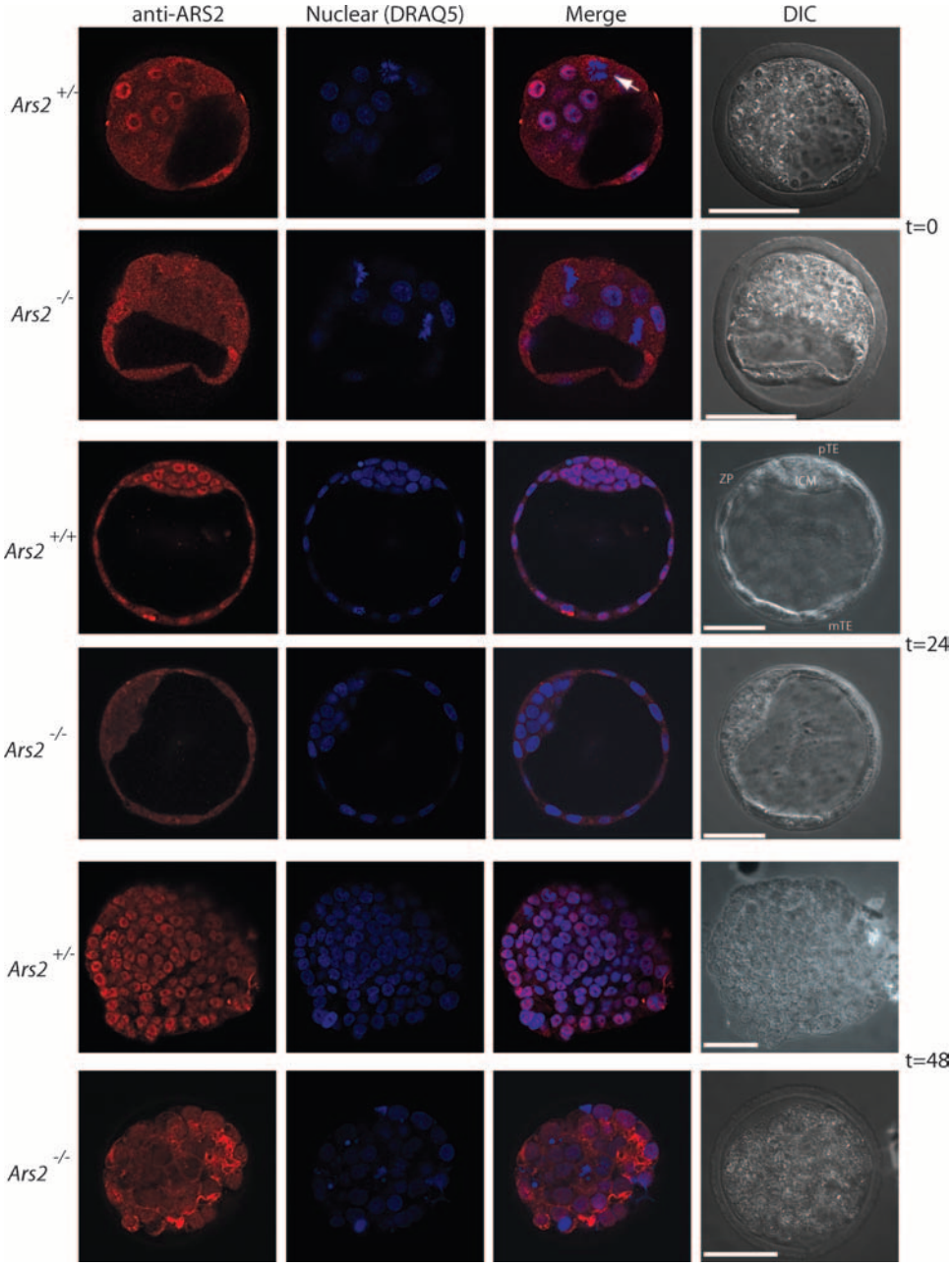

FIG. 6. ARS2 distribution in *ARS2*$^{+/+}$ *ARS2*$^{+/-}$ and *ARS2*$^{-/-}$ E3.5 embryos before and after 24 and 48 h of culture. Before culture (t = 0), the nuclear localization of ARS2 was detected with anti-ARS2 polyclonal antibody and Alexa Fluor 568 goat anti-rabbit IgG (red) in the wild type and was present in smaller amounts or even absent in null embryos. Nuclear DNA was stained using DRAQ5 (blue); the merge of red and blue and the differential interference microscopy (DIC) are indicated. Embryos were observed by confocal microscopy, and a representative single optical section is shown. At time zero, the arrow indicates the nuclear localization of ARS2 in a cell undergoing anaphase. After 24 h of culture (t = 24), both *ARS2*$^{+/-}$ and *ARS2*$^{-/-}$ embryos had formed expanded blastocysts and *ARS2*$^{-/-}$ embryos had completely lost their nuclear ARS2 localization. After 48 h of culture (t = 48), the null blastocyst had collapsed and several abnormal nuclei could be observed. The scale bars correspond to 50 μm.

"essential" genes, the onset of the *ARS2* mutant phenotype may have been delayed by maternal mRNA or protein stores (2, 31, 41).

A major challenge in cases of early embryonic lethality is to distinguish genes that are essential for cellular function from genes that are required for a developmental program. At E3.5, *ARS2*$^{-/-}$ embryos are defective and generally do not hatch from the zona pellucida and do not adhere well in culture, nor do they expand. *ARS2*$^{-/-}$ embryos contained both trophectoderm-positive (Cdx2) and ICM positive (Oct4) cells, suggesting that early cell fate determination was not affected. In contrast, *ARS2*$^{-/-}$ embryos displayed an increased level of apoptosis, suggesting ARS2 has an essential cellular function. The later, yet still developmentally related, pleiotropic phenotypes ob-

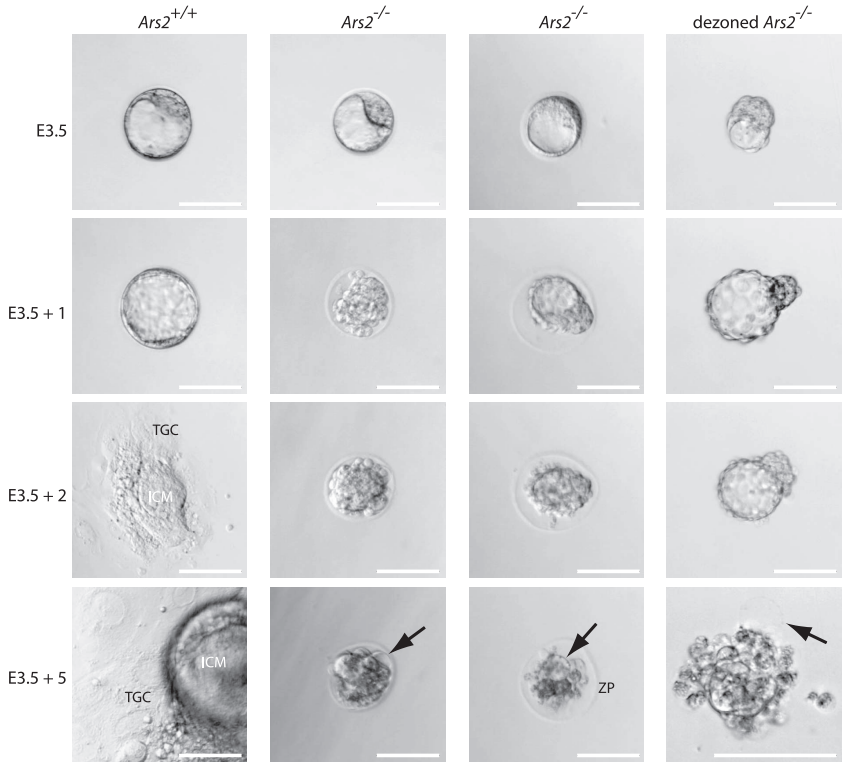

FIG. 7. Absence of blastocyst outgrowths in $ARS2^{-/-}$ embryos. Representative examples of cultured E3.5 blastocysts from $ARS2^{+/-}$ intercrosses are shown. The embryos were photographed every 24 h using phase-contrast microscopy. All embryos were genotyped after being cultured. At E3.5, no obvious differences between $ARS2^{+/+}$ $ARS2^{+/-}$ and $ARS2^{-/-}$ embryos were observed. By E3.5 plus 24 h (E3.5 + 1), some $ARS2^{-/-}$ embryos had collapsed and were generally not attached to the culture dish. $ARS2^{+/+}$ and $ARS2^{+/-}$ embryos had both expanded and attached by this time. By 48 h (E3.5 + 2), $ARS2^{+/+}$ and $ARS2^{+/-}$ embryos hatched from their zona pellucida (ZP), whereas $ARS2^{-/-}$ embryos invariably failed to hatch and were normally found floating in the medium or loosely attached to the gelatin-coated plates. The removal of the ZP in null blastocysts did not affect the phenotype (column 4). After 120 h (E3.5 + 5) of culture, $ARS2^{+/+}$ and $ARS2^{+/-}$ embryos were composed of outgrowths of ICM and were surrounded by a single layer of trophectoderm giant cells (TGC), whereas null embryos remained a small cluster of abnormal cells showing severe membrane blebbing (arrows).

served in zebrafish (11) and *Arabidopsis ARS2* mutants (25) indicate that these previously described random mutations were hypomorphic.

Several high-throughput screens have identified potential ARS2 protein partners. In a yeast two-hybrid screen using the transcription factor Rqcd1 (CG9573) as bait, the *Drosophila melanogaster ARS2* ortholog (CG7843) was identified as a Rqcd1 binding partner (10). Furthermore, chromatin immu-

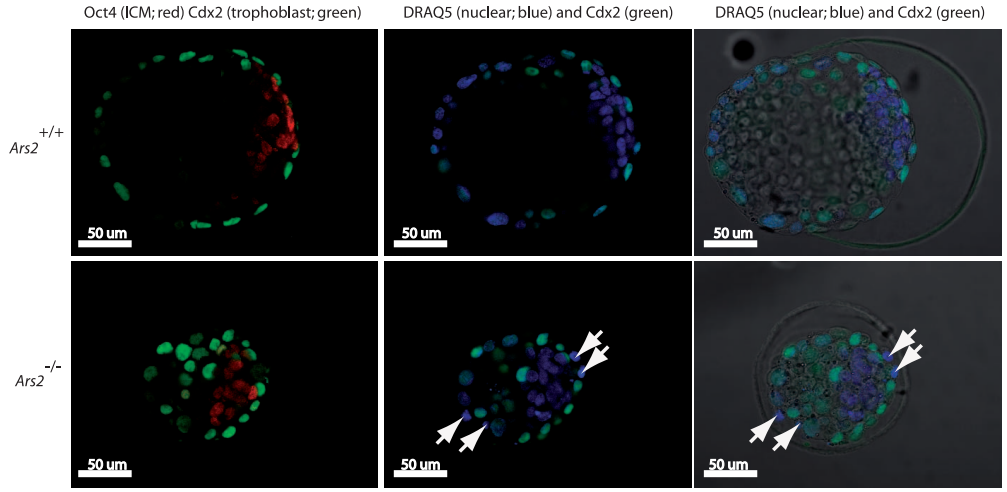

FIG. 8. Localization of the lineage-specific markers Cdx2 and Oct4 in $ARS2^{+/+}$ and $ARS2^{-/-}$ embryos. The trophectoderm marker Cdx2 was labeled with anti-CDX2 and Alexa Fluor 488 goat anti-mouse IgG (green). The ICM marker Oct4 was labeled with anti-OCT4 and Alexa Fluor 568 goat anti-rabbit IgG (red). Cells without either label showing condensed nuclei are indicated by arrows. The nuclei were labeled with DRAQ5 (blue). The embryos were observed by confocal microscopy, and a representative single optical section is shown.

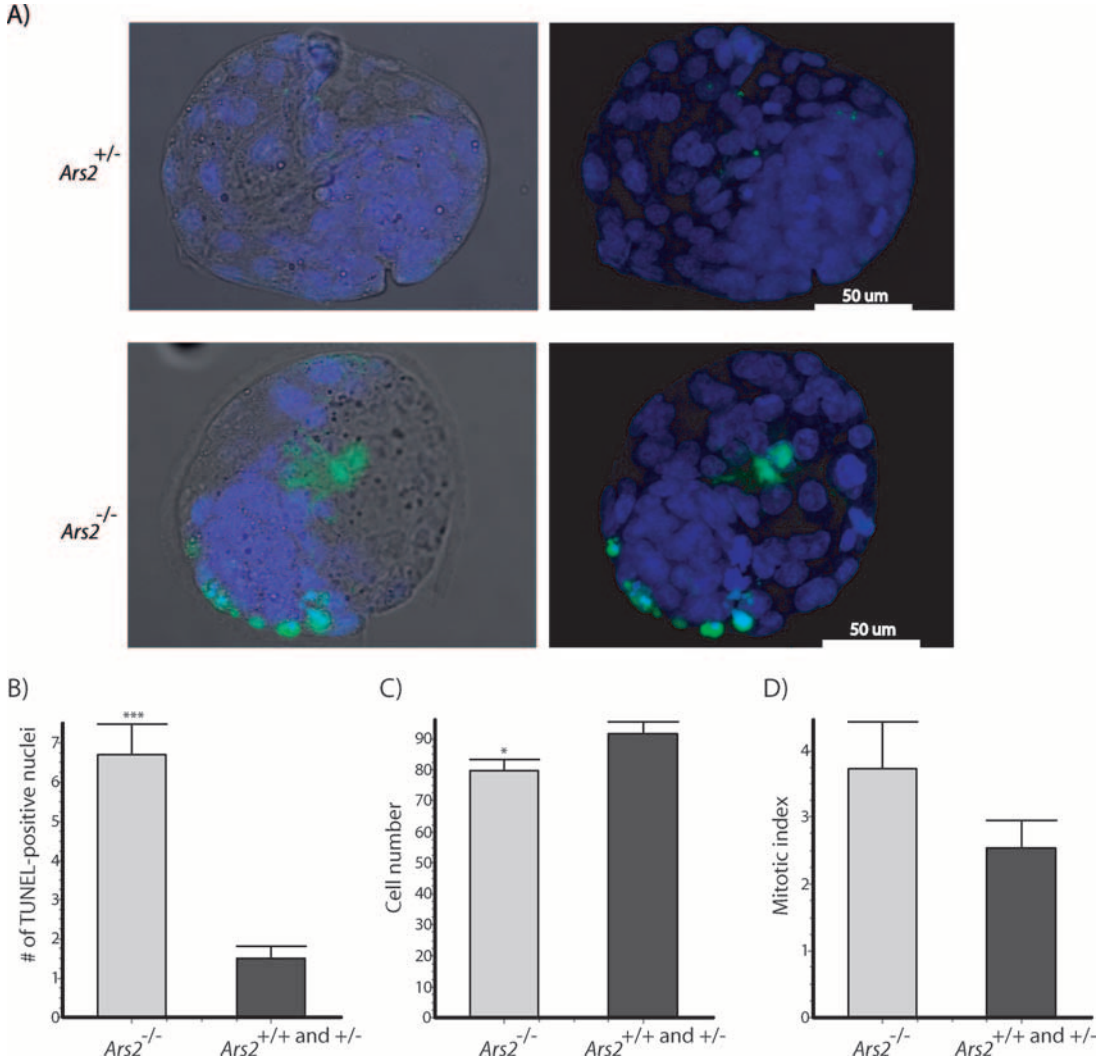

FIG. 9. Cultured *ARS2*-null embryos show excessive apoptosis. E3.5 blastocysts were cultured for 24 h, apoptotic cells were identified using a fluorescent TUNEL assay (green), and morphology was assessed with DRAQ5 nuclear stain (blue). The embryos were genotyped by PCR ($ARS2^{+/+}$ $ARS2^{+/-}$, $n = 12$; $ARS2^{-/-}$, $n = 7$). (A) A representative $ARS2^{-/-}$ embryo showing excessive TUNEL labeling predominantly in the trophectoderm and an $ARS2^{+/-}$ littermate. (B) There was a significant increase in TUNEL-positive nuclei in $ARS2^{-/-}$ over $ARS2^{+/+}$ $ARS2^{+/-}$ embryos ($t[28] = 7.4$; $P < 0.0001$). (C) Cell numbers in E3.5 embryos cultured for 24 h showed a statistically significant decrease in $ARS2^{-/-}$ cell numbers over $ARS2^{+/+}$ $ARS2^{+/-}$ E3.5 blastocysts cultured for 24 h ($t[38] = 2.3$; $P = 0.0283$). (D) No statistically significant difference in the mitotic index was observed between $ARS2^{+/+}$ $ARS2^{+/-}$ ($n = 12$) and $ARS2^{-/-}$ embryos ($t[10] = 1.45$; $P = 0.177$).

noprecipitation studies revealed that HNF4-alpha transcription factor bound to human *ARS2* and *RQCD1* promoters in the human adult liver (23), suggesting that *ARS2* and *RQCD1* are coregulated. In mammals, *Rqcd1* has been shown to mediate retinoic acid-induced cell differentiation in cell culture and mouse lung explants (15), and all trans-retinoic acid is used in conjunction with arsenic trioxide to treat acute promyelocytic leukemia (33). Based on these observations, we cloned the full-length mouse *Rcqd1* gene and performed coimmunoprecipitation by transfecting stable three-FLAG-*ARS2* or three-FLAG–*Rcqd1* cell lines with the Myc-His-tagged *ARS2* and *Rcqd1* genes. However, we did not detect any interaction between ARS2 and Rqcd1 in this system (data not shown).

More recently, human ARS2 has also been shown to interact with RNA binding protein S1 (RNPS1) in two separate high-throughput protein interaction studies, one in human kidney cells (7) and the other in a study directed at purified exon junction complexes from HeLa cells (36). RNPS1, which is responsible for regulating pre-mRNA splicing in vivo (29), was also shown to interact with SMN1 in a high-throughput protein interaction study by Ewing et al. (7). Importantly, Gemin4, an essential component of the SMN complex (4), also interacts with ARS2 (6). The SMN1 protein is the core of the SMN complex, and mutations in *SMN1* account for more than 98% of all spinal muscular atrophy cases (reviewed in reference 14). The SMN complex assembles Sm proteins onto the small nuclear RNAs, which in turn mediate pre-mRNA splicing. Gemin4 has been mapped to a minimum loss of heterozygosity region for hepatocellular carcinoma (43), and the ablation of

Gemin4 is sufficient to disrupt Sm core assembly (34). The independently confirmed protein-protein interaction between ARS2 and RNPS1, combined with their individual associations with components of the SMN complex, suggests that ARS2 may play a role in some aspect of RNA metabolism. Importantly the inactivation of the mouse *Smn1* gene resulted in a phenotype similar to that of our *ARS2*-null mice; most notably, the formation of disorganized multicystic structures, extensive cellular degeneration, and massive cell death due to apoptosis are shared between *Smn1* and *ARS2* mutants (31). In addition, the ablation of the Smn1-interacting zinc finger protein Zpr1 also resulted in a similar early embryonic-lethal phenotype with increased apoptosis and lack of proliferation in embryonic tissues (9). Clearly, determining whether *ARS2* is involved in RNA metabolism will be important in the future. In addition to RNPS1 and Gemin4, five human ARS2-interacting proteins have been reported (chromodomain helicase-DNA-binding protein 3 [CHD3], ARF GTPase-activating protein [GIT1], vimentin [VIM], mitochondrial inner membrane protein [IMMT], and small ubiquitin-related modifier 2 precursor [SUMO2]) (35). The significance of these interactions remains to be determined.

Consistent with a putative role in RNA metabolism, recent studies of the *Arabidopsis ARS2* ortholog *SERRATE* (*SE*) demonstrated that *SE* plays a general role in processing primary microRNA transcripts (12, 17, 42). *SE* has also been shown to colocalize to nuclear dicing bodies containing proteins essential for microRNA processing in *Arabidopsis* (8). While studies in plants convincingly show that *SE* is involved in microRNA processing, this role in animals has yet to be demonstrated. In the context of arsenite resistance, it has recently been shown that treatment of the human lymphoblast line TK-6 with sodium arsenite led to a global increase in microRNA expression due to a lack of proper precursor processing (18). This finding is particularly intriguing in light of *SE*'s essential role in processing *Arabidopsis* microRNAs. Whether the role of *ARS2* in arsenic resistance is related to some aspect of posttranscriptional regulation remains to be seen.

The loss of single-copy proteins conserved throughout the *Eukaryota* would be predicted to result in early and severe developmental phenotypes. Here, we performed an in vivo analysis of the *ARS2* gene, and we show that abolishing the nuclear expression of ARS2 leads to peri-implantation lethality with an increase in apoptosis and a decrease in cell numbers. These data show that *ARS2* is involved in an essential cellular process required for the development of diverse eukaryotic organisms. *ARS2* resides in one of the regions within 7q22 that is recurrently deleted in acute myeloid leukemia (reviewed in reference 30). However, we observed no obvious phenotype in $ARS2^{+/-}$ blastocysts and adult mice (data not shown), suggesting that the haploinsufficiency of *ARS2* alone is not enough to cause disease. Because of the early lethality, we could not examine the role of *ARS2*-null mutations in adult tissues. *SERRATE*'s role in microRNA processing in *Arabidopsis* and ARS2's association with mammalian proteins involved in pre-mRNA splicing are intriguing, and future studies of *ARS2* may be relevant not only to arsenic resistance and cancer, but also to other human diseases.

ACKNOWLEDGMENTS

We thank Stacy Lew and Raymond Wong for making the aggregation chimeras, Daniel Morgado for animal care assistance, Jill Brandon for BOSC cell transfection, Bob Chow and Haiquan Liu for use of and advice on confocal microscopy, Brent Gowen for serial embryo sectioning, and Yojiro Yamanaka and Claudia Kutter for helpful discussions.

This work was supported by an NSERC grant to B.F.K. and a Michael Smith Foundation for Health Research trainee award to M.D.W.

REFERENCES

1. **Amsterdam, A., R. M. Nissen, Z. Sun, E. C. Swindell, S. Farrington, and N. Hopkins.** 2004. Identification of 315 genes essential for early zebrafish development. Proc. Natl. Acad. Sci. USA **101:**12792–12797.
2. **Artus, J., S. Vandormael-Pournin, M. Frodin, K. Nacerddine, C. Babinet, and M. Cohen-Tannoudji.** 2005. Impaired mitotic progression and preimplantation lethality in mice lacking OMCG1, a new evolutionarily conserved nuclear protein. Mol. Cell. Biol. **25:**6289–6302.
3. **Blanchette, M., W. J. Kent, C. Riemer, L. Elnitski, A. F. A. Smit, K. M. Roskin, R. Baertsch, K. Rosenbloom, H. Clawson, E. D. Green, D. Haussler, and W. Miller.** 2004. Aligning multiple genomic sequences with the threaded blockset aligner. Genome Res. **14:**708–715.
4. **Charroux, B., L. Pellizzoni, R. A. Perkinson, J. Yong, A. Shevchenko, M. Mann, and G. Dreyfuss.** 2000. Gemin4: a novel component of the SMN complex that is found in both gems and nucleoli. J. Cell Biol. **148:**1177–1186.
5. **Clarke, J. H., D. Tack, K. Findlay, M. Van Montagu, and M. Van Lijsebettens.** 1999. The SERRATE locus controls the formation of the early juvenile leaves and phase length in *Arabidopsis*. Plant J. **20:**493–501.
6. **Di, Y., J. Li, Y. Zhang, X. He, H. Lu, D. Xu, J. Ling, K. Huo, D. Wan, Y. Y. Li, and J. Gu.** 2003. HCC-associated protein HCAP1, a variant of GEMIN4, interacts with zinc-finger proteins. J. Biochem. (Tokyo) **133:**713–718.
7. **Ewing, R. M., P. Chu, F. Elisma, H. Li, P. Taylor, S. Climie, L. McBroom-Cerajewski, M. D. Robinson, L. O'Connor, M. Li, R. Taylor, M. Dharsee, Y. Ho, A. Heilbut, L. Moore, S. Zhang, O. Ornatsky, Y. V. Bukhman, M. Ethier, Y. Sheng, J. Vasilescu, M. Abu-Farha, J. P. Lambert, H. S. Duewel, I. I. Stewart, B. Kuehl, K. Hogue, K. Colwill, K. Gladwish, B. Muskat, R. Kinach, S. L. Adams, M. F. Moran, G. B. Morin, T. Topaloglou, and D. Figeys.** 2007. Large-scale mapping of human protein-protein interactions by mass spectrometry. Mol. Syst. Biol. **3:**89.
8. **Fang, Y., and D. Spector.** 2007. Identification of nuclear dicing bodies containing proteins for microRNA biogenesis in living *Arabidopsis* plants. Curr. Biol. **17:**818–823.
9. **Gangwani, L., R. A. Flavell, and R. J. Davis.** 2005. ZPR1 is essential for survival and is required for localization of the survival motor neurons (SMN) protein to Cajal bodies. Mol. Cell. Biol. **25:**2744–2756.
10. **Giot, L., J. S. Bader, C. Brouwer, A. Chaudhuri, B. Kuang, Y. Li, Y. L. Hao, C. E. Ooi, B. Godwin, E. Vitols, G. Vijayadamodar, P. Pochart, H. Machineni, M. Welsh, Y. Kong, B. Zerhusen, R. Malcolm, Z. Varrone, A. Collis, M. Minto, S. Burgess, L. McDaniel, E. Stimpson, F. Spriggs, J. Williams, K. Neurath, N. Ioime, M. Agee, E. Voss, K. Furtak, R. Renzulli, N. Aanensen, S. Carrolla, E. Bickelhaupt, Y. Lazovatsky, A. DaSilva, J. Zhong, C. A. Stanyon, R. L. Finley, Jr., K. P. White, M. Braverman, T. Jarvie, S. Gold, M. Leach, J. Knight, R. A. Shimkets, M. P. McKenna, J. Chant, and J. M. Rothberg.** 2003. A protein interaction map of *Drosophila melanogaster*. Science **302:**1727–1736.
11. **Golling, G., A. Amsterdam, Z. Sun, M. Antonelli, E. Maldonado, W. Chen, S. Burgess, M. Haldi, K. Artzt, S. Farrington, S. Y. Lin, R. M. Nissen, and N. Hopkins.** 2002. Insertional mutagenesis in zebrafish rapidly identifies genes essential for early vertebrate development. Nat. Genet. **31:**135–140.
12. **Grigg, S., C. Canales, A. Hay, and M. Tsiantis.** 2005. SERRATE coordinates shoot meristem function and leaf axial patterning in *Arabidopsis*. Nature **437:**1022–1026.
13. **Groot, E. P., and R. D. Meicenheimer.** 2000. Comparison of leaf plastochron index and allometric analyses of tooth development in *Arabidopsis thaliana*. J. Plant Growth Regul. **19:**77–89.
14. **Gubitz, A. K., W. Feng, and G. Dreyfuss.** 2004. The SMN complex. Exp. Cell Res. **296:**51–56.
15. **Hiroi, N., T. Ito, H. Yamamoto, T. Ochiya, S. Jinno, and H. Okayama.** 2002. Mammalian Rcd1 is a novel transcriptional cofactor that mediates retinoic acid-induced cell differentiation. EMBO J. **21:**5235–5244.
16. **Joyner, A. L.** 2000. Gene targeting: a practical approach, 2nd ed. Oxford University Press, Oxford, NY.
17. **Lobbes, D., G. Rallapalli, D. Schmidt, C. Martin, and J. Clarke.** 2006. SERRATE: a new player on the plant microRNA scene. EMBO Rep. **7:**1052–1058.
18. **Marsit, C. J., K. Eddy, and K. T. Kelsey.** 2006. MicroRNA responses to cellular stress. Cancer Res. **66:**10843–10848.
19. **Nagy, A.** 2000. Cre recombinase: the universal reagent for genome tailoring. Genesis **26:**99–109.

20. **Nagy, A.** 2003. Manipulating the mouse embryo: a laboratory manual, 3rd ed. Cold Spring Harbor Laboratory Press, Cold Spring Harbor, NY.
21. **Nagy, A., J. Rossant, R. Nagy, W. Abramow-Newerly, and J. C. Roder.** 1993. Derivation of completely cell culture-derived mice from early-passage embryonic stem cells. Proc. Natl. Acad. Sci. USA **90:**8424–8428.
22. **Ng, J. C.** 2005. Environmental contamination of arsenic and its toxicological impact on humans. Environ. Chem. **2:**146–160.
23. **Odom, D. T., N. Zizlsperger, D. B. Gordon, G. W. Bell, N. J. Rinaldi, H. L. Murray, T. L. Volkert, J. Schreiber, P. A. Rolfe, D. K. Gifford, E. Fraenkel, G. I. Bell, and R. A. Young.** 2004. Control of pancreas and liver gene expression by HNF transcription factors. Science **303:**1378–1381.
24. **Ori, N., Y. Eshed, G. Chuck, J. L. Bowman, and S. Hake.** 2000. Mechanisms that control knox gene expression in the *Arabidopsis* shoot. Development **127:**5523–5532.
25. **Prigge, M. J., and D. R. Wagner.** 2001. The arabidopsis serrate gene encodes a zinc-finger protein required for normal shoot development. Plant Cell **13:**1263–1279.
26. **Ramirez-Solis, R., J. Rivera-Perez, J. D. Wallace, M. Wims, H. Zheng, and A. Bradley.** 1992. Genomic DNA microextraction: a method to screen numerous samples. Anal. Biochem. **201:**331–335.
27. **Rossman, T. G.** 2003. Mechanism of arsenic carcinogenesis: an integrated approach. Mutat. Res. **533:**37–65.
28. **Rossman, T. G., and Z. Wang.** 1999. Expression cloning for arsenite-resistance resulted in isolation of tumor-suppressor fau cDNA: possible involvement of the ubiquitin system in arsenic carcinogenesis. Carcinogenesis **20:** 311–316.
29. **Sakashita, E., S. Tatsumi, D. Werner, H. Endo, and A. Mayeda.** 2004. Human RNPS1 and its associated factors: a versatile alternative pre-mRNA splicing regulator in vivo. Mol. Cell. Biol. **24:**1174–1187.
30. **Scherer, S. W., and E. D. Green.** 2004. Human chromosome 7 circa 2004: a model for structural and functional studies of the human genome. Hum. Mol. Genet. **13:**R303–R313.
31. **Schrank, B., R. Gotz, J. M. Gunnersen, J. M. Ure, K. V. Toyka, A. G. Smith, and M. Sendtner.** 1997. Inactivation of the survival motor neuron gene, a candidate gene for human spinal muscular atrophy, leads to massive cell death in early mouse embryos. Proc. Natl. Acad. Sci. USA **94:**9920–9925.
32. **Serrano-Cartagena, J., P. Robles, M. R. Ponce, and J. L. Micol.** 1999. Genetic analysis of leaf form mutants from the Arabidopsis Information Service collection. Mol. Gen. Genet. **261:**725–739.
33. **Shen, Z. X., Z. Z. Shi, J. Fang, B. W. Gu, J. M. Li, Y. M. Zhu, J. Y. Shi, P. Z. Zheng, H. Yan, Y. F. Liu, Y. Chen, Y. Shen, W. Wu, W. Tang, S. Waxman, H. De The, Z. Y. Wang, S. J. Chen, and Z. Chen.** 2004. All-trans retinoic acid/As2O3 combination yields a high quality remission and survival in newly diagnosed acute promyelocytic leukemia. Proc. Natl. Acad. Sci. USA **101:** 5328–5335.
34. **Shpargel, K. B., and A. G. Matera.** 2005. Gemin proteins are required for efficient assembly of Sm-class ribonucleoproteins. Proc. Natl. Acad. Sci. USA **102:**17372–17377.
35. **Stelzl, U., U. Worm, M. Lalowski, C. Haenig, F. H. Brembeck, H. Goehler, M. Stroedicke, M. Zenkner, A. Schoenherr, S. Koeppen, J. Timm, S. Mintzlaff, C. Abraham, N. Bock, S. Kietzmann, A. Goedde, E. Toksoz, A. Droege, S. Krobitsch, B. Korn, W. Birchmeier, H. Lehrach, and E. E. Wanker.** 2005. A human protein-protein interaction network: a resource for annotating the proteome. Cell **122:**957–968.
36. **Tange, T. O., T. Shibuya, M. S. Jurica, and M. J. Moore.** 2005. Biochemical analysis of the EJC reveals two new factors and a stable tetrameric protein core. RNA **11:**1869–1883.
37. **Verstovsek, S. F. Giles, A. Quintás-Cardama, N. Perez, F. Ravandi-Kashani, M. Beran, E. Freireich, and H. Kantarjian.** 2006. Arsenic derivatives in hematologic malignancies: a role beyond acute promyelocytic leukemia? Hematol. Oncol. **24:**181–188.
38. **Waxman, S., and K. C. Anderson.** 2001. History of the development of arsenic derivatives in cancer therapy. Oncologist **6**(Suppl. 2)**:**3–10.
39. **Wheeler, D. L., D. M. Church, S. Federhen, A. E. Lash, T. L. Madden, J. U. Pontius, G. D. Schuler, L. M. Schriml, E. Sequeira, T. A. Tatusova, and L. Wagner.** 2003. Database resources of the National Center for Biotechnology. Nucleic Acids Res. **31:**28–33.
40. **Wilson, M. D., C. Riemer, D. W. Martindale, P. Schnupf, A. P. Boright, T. L. Cheung, D. M. Hardy, S. Schwartz, S. W. Scherer, L. C. Tsui, W. Miller, and B. F. Koop.** 2001. Comparative analysis of the gene-dense ACHE/TFR2 region on human chromosome 7q22 with the orthologous region on mouse chromosome 5. Nucleic Acids Res. **29:**1352–1365.
41. **Xie, Y., Y. Wang, T. Sun, F. Wang, A. Trostinskaia, E. Puscheck, and D. A. Rappolee.** 2005. Six post-implantation lethal knockouts of genes for lipophilic MAPK pathway proteins are expressed in preimplantation mouse embryos and trophoblast stem cells. Mol. Reprod. Dev. **71:**1–11.
42. **Yang, L., Z. Liu, F. Lu, A. Dong, and H. Huang.** 2006. SERRATE is a novel nuclear regulator in primary microRNA processing in *Arabidopsis*. Plant J. **47:**841–850.
43. **Zhao, X., M. He, D. Wan, Y. Ye, Y. He, L. Han, M. Guo, Y. Huang, W. Qin, M.-W. Wang, W. Chong, J. Chen, L. Zhang, N. Yang, B. Xu, M. Wu, L. Zuo, and J. Gu.** 2003. The minimum LOH region defined on chromosome 17p13.3 in human hepatocellular carcinoma with gene content analysis. Cancer Lett. **190:**221–232.